Gondwana Research 121 (2023) 368–382

Contents lists available at ScienceDirect

Gondwana Research

journal homepage: www.elsevier.com/locate/gr

Linking accretionary orogens with continental crustal growth and stabilization: Lessons from Patagonia

Sebastián Oriolo [a,*], Pablo D. González [b], Emiliano M. Renda [c], Miguel A.S. Basei [d], Juan Otamendi [e], Pablo Cordenons [a], Paulo Marcos [c], María Belén Yoya [a], Carlos A. Ballivián Justiniano [a], Rodrigo Suárez [c]

[a] CONICET-Universidad de Buenos Aires, Instituto de Geociencias Básicas, Aplicadas y Ambientales de Buenos Aires (IGEBA), Intendente Güiraldes 2160, C1428EHA Buenos Aires, Argentina
[b] CONICET-SEGEMAR, Regional Sur, Independencia 1495, Parque Industrial 1, R8332EXZ General Roca, Argentina
[c] Instituto de Investigación en Paleobiología y Geología (UNRN-CONICET), Avenida Julio A. Roca 1242, R8332EXZ General Roca, Argentina
[d] Centro de Pesquisas Geocronologicas, Instituto de Geociências, Universidade de São Paulo, Rua do Lago 562, CEP 05508-080 São Paulo, Brazil
[e] CONICET, Departamento de Geología, Universidad Nacional de Río Cuarto, Campus Universitario, X5804BYA Río Cuarto, Argentina

ARTICLE INFO

Article history:
Received 9 February 2023
Revised 24 April 2023
Accepted 21 May 2023
Available online 23 May 2023
Handling Editor: Andrea Festa

Keywords:
Magmatic arc dynamics
Crustal stabilization
Crustal thickening and thinning
Paleozoic
Gondwanide Orogeny
Terra Australis Orogen

ABSTRACT

The origin of the continental crust and the tectonic significance of Paleozoic magmatic rocks of Patagonia (southernmost South America) remain one of the main enigmas in the history of the Gondwana supercontinent. Here, new whole-rock geochemistry together with coupled zircon U-Pb and Lu-Hf isotopic data of Devonian to Permian intrusive rocks of northern Patagonia are integrated with a revised geochemical and isotopic database of the region, providing a novel model for the tectonomagmatic evolution and related crustal growth mechanisms. The development of a Devonian retreating accretionary orogen associated with crustal thinning was succeeded by a late Carboniferous to Permian advancing orogen and crustal shortening, resulting from slab shallowing. The latter was related to the Gondwanide Orogeny, a major transpressional tectonic event that led to the maturation and stabilization of the continental crust of Patagonia due to widespread magmatism and crustal thickening, which culminated with Permian-Triassic slab break-off. Addition of juvenile mantle-derived magmas is more significant during the Devonian, whereas a progressively increase in crustal reworking is documented from the late Carboniferous to the Permian due to crustal thickening. Therefore, this non-collisional model favors an *in situ* middle to late Paleozoic crustal growth of Patagonia during changing dynamics of accretionary orogens at the proto-Pacific margin of southwestern Gondwana.

1. Introduction

Assessing the geodynamic evolution of accretionary orogens is crucial to understand continental crustal growth (Condie, 2007). Accretionary orogens result from subduction along convergent margins and can be subdivided into advancing and retreating types, depending on whether they are associated with compression/transpression or extension/transtension, respectively (Cawood et al., 2009). Crustal addition is dominant in retreating-mode accretionary orogens, where crustal extension/transtension favors the *in situ* emplacement of juvenile mantle-derived magmas (Collins, 2002; Cawood et al., 2009; Kemp et al., 2009). Nevertheless, *ex situ* mechanisms, such as the accretion of oceanic rocks (e.g., island arc complexes, oceanic plateaus, aseismic ridges), also facilitate incorporation of juvenile material in advancing orogens (e.g., Cawood et al., 2009). Besides *in situ* and *ex situ* mechanisms, incorporation of mantle-derived magmas occurs in all continental magmatic arcs to some extent, independently of their association with advancing- or retreating-type accretionary orogens (Kemp et al., 2009). These magmas ultimately result in widespread calc-alkaline, dominantly intermediate magmatic suites in continental arcs, achieved by a complex interaction of fractionation, melting and assimilation processes (Ducea et al., 2015; Moyen et al., 2017). Fractionation gives rise to emplacement of nearly juvenile intrusions and, therefore, addition of newly formed crust, whereas melting and assimilation imply partial reworking of pre-existing crust (Moyen et al., 2017).

In the last years, geochemical proxies such as Sr/Y, La_N/Yb_N and Eu/Eu* have arisen as powerful tools to identify periods of crustal thickening and thinning in orogens (Chapman et al., 2015; Chiaradia, 2015; Profeta et al., 2015; Tang et al., 2021). These

* Corresponding author.
E-mail address: soriolo@gl.fcen.uba.ar (S. Oriolo).

https://doi.org/10.1016/j.gr.2023.05.011
1342-937X/

parameters are essentially based on differential element partitioning among key minerals, whose presence in the magma source is controlled by depth and, consequently, by crustal thickness. For instance, plagioclase incorporates Sr from evolving magmatic melts over its wide stability field at relatively low crustal pressures, whereas Y shows an incompatible behavior at such conditions (e.g., Profeta et al. 2015). Therefore, plagioclase fractionation in shallow sources is commonly documented by both low Sr/Y and negative Eu/Eu* (Eu anomaly) values (e.g., Dessimoz et al. 2012). As pressure increases, however, plagioclase becomes unstable and Sr is storaged in the melt. In turn, fractionation of both amphibole and garnet partitions Y (Gaetani et al., 2003; Nandedkar et al., 2016), thus leading to increasing Sr/Y in melts. La/Yb also increases at increasing pressures, mainly due to the compatible behavior of Yb during garnet fractionation (Gaetani et al., 2003, and references therein).

Comparably, Lu-Hf isotopic trends of zircons also provide robust evidence of orogenic evolution, allowing the discrimination between juvenile mantle-derived magmas and those dominated by crustal reworking, which can in turn be linked to periods of crustal thinning and thickening, respectively (e.g., Collins et al., 2011; Spencer et al., 2019). Juvenile mantle-derived magmas are governed by suprachondritic isotopic compositions. However, the isotopic fingerprint tends towards subchondritic ε_{Hf} values with increasing proportions of recycled continental crust, which is in turn favored by thicker continental crust (e.g., Chapman et al., 2017).

On the other hand, spatial and temporal variations in arc dynamics are critical for the growth and stabilization of the continental crust. Protracted subduction along accretionary orogens leads to a progressive growth of the continental crust, which is finally stabilized during compression/transpression, resulting in crustal thickening and significant magma addition (e.g., Cawood et al., 2009). Therefore, the final architecture of subduction-related orogens is mainly a consequence of alternating periods of crustal thickening and thinning related to episodic flare-up events and variable magmatic addition rates (Haschke and Gunther, 2003; Paterson and Ducea, 2015).

The Paleozoic orogenic evolution of Patagonia (southernmost South America) is one of the most controversial topics in the geodynamic context of Western Gondwana. The construction of this crustal segment has alternatively been interpreted as the result of either collisional or accretionary processes. Collisional models have postulated the Paleozoic assembly of one or more crustal blocks (e.g., North Patagonian Massif, Deseado Massif, Antarctic Peninsula) to the proto-Pacific margin of western Gondwana (Pankhurst et al., 2006; Ramos, 2008; Martínez et al., 2012; González et al., 2018; Heredia et al., 2018). In contrast, accretionary models have inferred diverse mechanisms, involving subduction under changing geodynamic conditions and associated accretion of forearc sequences, oceanic rocks and/or island arc complexes (Forsythe, 1982; Hervé et al., 2016; Oriolo et al., 2019; Marcos et al., 2020; Rapela et al., 2021). In any case, the magmatic evolution of Devonian to Permian arc-related intrusions is a key element to assess middle to late Paleozoic tectonic processes of Patagonia, which are particularly well-recorded between the North Patagonian Andes (NPA) and the North Patagonian Massif (NPM) (Fig. 1; Varela et al., 2005, 2015; Pankhurst et al., 2006; Rapela et al., 2021; Serra-Varela et al., 2021).

In this contribution, new whole-rock geochemical and coupled U-Pb and Lu-Hf zircon isotopic data of arc-related Devonian to Permian intrusions of northern Patagonia are provided and integrated with geochemical and isotopic data from the literature. Results are evaluated to analyze spatial and temporal variations in the Devonian to Permian tectonomagmatic evolution of Patagonia. In particular, the role of changing tectonic regimes of Paleozoic accretionary orogens and resulting large-scale magmatic arc dynamics are revised. A model of incremental continental crustal growth during protracted accretionary processes is finally presented for Patagonia, thus challenging collisional models for the region.

2. Geologic setting

Devonian to Permian intrusions, mainly corresponding to arc-related magmatism, are widespread in northern Patagonia (Fig. 1). Remarkably, both Devonian and late Carboniferous-early Permian magmatic systems are mainly exposed in a similar position between the NPA and the western NPM, though middle to late Permian intrusions are widespread further east (Fig. 1; e.g., Pankhurst et al., 2006; Martínez Dopico et al., 2017; Renda et al., 2019; Gregori et al., 2021; Serra-Varela et al., 2021). A period of ca. 20 My of magmatic quiescence separates the Devonian magmatism from a protracted late Carboniferous-Permian magmatic cycle related to the Gondwanide Orogeny (Renda et al., 2021), thus indicating that they represent two different pulses (Varela et al., 2005, 2015; Pankhurst et al., 2006; Rapela et al., 2021; Renda et al., 2021; Serra-Varela et al., 2021). A singular expression of Devonian magmatism, however, occurs further southwest in the Pacific Domain (PD) of southern Chile, which shows a distinct geochemical and isotopic signature in close association with oceanic metamorphic rocks (Hervé et al., 2016; Rapela et al., 2021).

Devonian intrusions in the NPA are associated with coeval regional medium- to high-grade metamorphism, typically under low-pressure conditions up to ca. 4–5 kbar (Martínez et al., 2012; Serra-Varela et al., 2019). In contrast, medium- to high-pressure peak conditions (ca. 6–11 kbar) characterize late Carboniferous-early Permian medium- to high-grade metamorphism and deformation, well-documented in the wall rock of coeval intrusions between the NPA and the western NPM (Marcos et al., 2020; Oriolo et al., 2019; Renda et al., 2021; von Gosen, 2009).

In a similar way to the igneous record, regional metamorphism and deformation are younger to the east, with middle to late Permian ages in the eastern NPM (e.g., von Gosen, 2003; Martínez Dopico et al., 2017). Permian low-grade metamorphism and deformation, together with coeval volcaniclastic sequences, are also well-documented further northeast in the Sierras Australes (e.g., von Gosen, 2003; Ballivián Justiniano et al., 2023). In addition, the eastern NPM hosts relics of Cambrian to Ordovician tectonomagmatic and metamorphic processes (Pankhurst et al., 2006, 2014; González et al., 2018, 2021).

3. Materials and methods

Five new samples of key basement intrusions were analyzed using whole-rock geochemistry and coupled zircon U-Pb and Lu-Hf LA-ICP-MS isotopic analysis (Fig. 1). For the geochemical characterization, whole-rock analyses were carried out at AcmeLabs, Canada (https://acmelab.com/), using Lithoborate fusion and ICP-ES (major and minor elements) and ICP-MS (trace and rare earth elements) methods. All geochemical data were analyzed using the GCDkit 4.1 software (Janoušek et al., 2006, 2016). On the other hand, zircon U-Pb and Lu-Hf isotopic analyses were carried out at the Geochronological Research Centre of the University of São Paulo (Brazil) using a Thermo Fisher Scientific Neptune multicollector inductively coupled plasma – mass spectrometer (ICP-MS). Analytical protocols and results are included in Supplementary Data (File S1, and Tables S1 and S2).

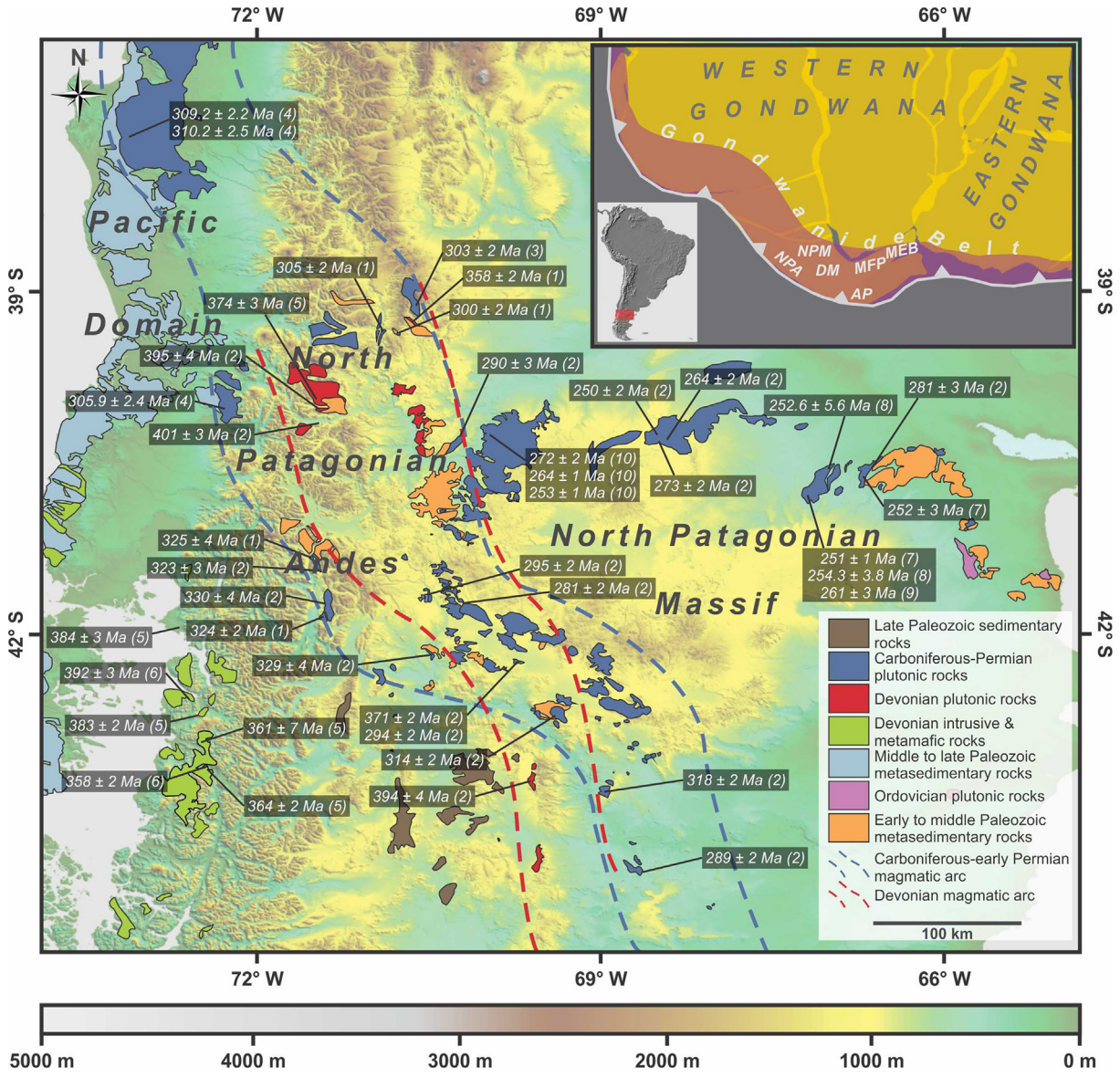

Fig. 1. Sketch map showing distribution of igneous and metamorphic basement rocks of northern Patagonia (modified after Pankhurst et al., 2006; Ramos, 2008; Hervé et al., 2016; González et al., 2018; Renda et al., 2019; Serra-Varela et al., 2021). The inset indicates location of the study area and simplified Late Paleozoic paleogeography of Gondwana. NPM: North Patagonian Massif, NPA: North Patagonian Andes, DM: Deseado Massif, AP: Antarctic Peninsula, MFP: Malvinas/Falkland Plateau, MEB: Maurice Ewing Bank. Representative zircon U-Pb SHRIMP and LA-ICP-MS ages of Devonian to Permian intrusions are also shown (1: this work, 2: Pankhurst et al., 2006; 3: Romero et al., 2020; 4: Deckart et al., 2014; 5: Hervé et al., 2016; 6: Rapela et al., 2021; 7: Pankhurst et al., 2014; 8: Martínez Dopico et al., 2017; 9: Chernicoff et al., 2013; 10: Gregori et al., 2021).

4. Results

4.1. Geochronology

Sample RA 5–18 (39°24′37.5″S, 70°48′14.2″W) corresponds to an equigranular granodiorite that intrudes metasedimentary sequences yielding Ordovician maximum deposition ages at Cuesta de Rahue (Hervé et al., 2018; Oriolo et al., 2023). This intrusion is composed of quartz, plagioclase, K-feldspar and biotite, and yields a concordia age of 300 ± 4 Ma (2σ, 11 out of 24 spots, MSWD = 0.61; Supplementary Data, Table S2), in line with the age of 306 ± 2 Ma reported for an associated dyke (Hervé et al., 2018). Immediately further west, sample RA 10–18 (39°22′08.4″S, 70°55′49.9″W) was collected at the Rahue locality. This equigranular quartz diorite comprises plagioclase, quartz, biotite, hornblende and clinopyroxene. The obtained concordia age of 305 ± 2 Ma (2σ, 19 out of 24 zircons, MSWD = 0.81; Supplementary Data, Table S2) is comparable with previous Rb-Sr isochrones ages of ca. 300 Ma (Lucassen et al., 2004).

Further southwest, two samples (BA 33–17 and SE 8–19) of quartz diorites intercalated with subordinate gabbros were obtained. Sample BA 33–17 was collected at the margin of Guillelmo lake (41°22′19.1″S, 71°30′40.2″W), whereas SE-8–19 (41°56′51.9″S, 71°23′30.5″W) corresponds to rocks exposed at Morro de Sheffield (Yoya et al., 2023). These diorites are made up of plagioclase, hornblende, quartz and scarce biotite, and yield within-error undistinguishable concordia ages of 325 ± 4 (BA 33–17, 2σ, 14 out 24 spots, MSWD = 0.84) and 324 ± 2 (SE 8-19A, 2σ, 13 out 24 spots, MSWD = 1.60) Ma (Supplementary Data, Table S2). Comparable zircon U-Pb SHRIMP ages of 323 ± 3 (Cañadón de la Mosca) and 330 ± 4 (Cordón del Serrucho) Ma were previously reported for spatially associated intrusions (Pankhurst et al., 2006; Yoya et al., 2023).

Finally, sample RA 48–18 (39°20′40.4″S, 70°39′12.3″W) comprises a porphyritic granite constituted by quartz, K-feldspar, plagioclase and very minor biotite, which intrudes metasedimentary rocks of the Piedra Santa Complex at the Catán Lil creek (Franzese, 1995). A concordia age of 358 ± 2 Ma was obtained for this sample (2σ, 9 out of 24 spots, MSWD = 0.39; Supplementary Data, Table S2).

4.2. Geochemical characterization of the magmatic source

New geochemical and geochronologic data (Supplementary Data, Files S1 and Tables S1 and S2) were integrated with published data of northern Patagonian Devonian to Permian intrusions. Since Devonian and late Carboniferous-Permian magmatic pulses are separated by a period of ca. 20 My of magmatic quiescence, these age groups are separated for the analysis. In addition, Devonian rocks of the PD are also discriminated due to their singular geochemical and isotopic affinity in close association with oceanic rocks (see below). The database comprises a total of n = 95 samples, including five samples from this study, from which a low-silica subset (SiO_2 < 60 wt% and #Mg = 40–70, with #Mg = 1 00.MgO/MgO + FeO based on molar contents) was selected for detailed analysis. These gabbroic to dioritic rocks match primitive arc magma compositions (Schmidt and Jagoutz, 2017), which are more representative of the mantle and deep crustal sources. This aspect is particularly relevant since the studied plutons intrude Paleozoic metasedimentary sequences (Varela et al., 2005, 2015; Pankhurst et al., 2006; Serra-Varela et al., 2021), which are likely to have affected the geochemical fingerprint due to assimilation and/or anatexis. For this reason, rocks with a clear anatectic origin were not included in the database.

Devonian to Permian intrusions comprise a calc-alkaline suite that encompasses gabbroic to granitic with dominantly magnesian, calcic to calc-alkalic, and meta- to peraluminous compositions (Figs. 2, 3). As a whole, this geochemical fingerprint documents a magmatic arc signature (Pankhurst et al., 2006; Ramos, 2008; Varela et al., 2015; Hervé et al., 2016; Rapela et al., 2021; Serra-Varela et al., 2021). In the Nb/Yb *vs* Th/Yb diagram, the composition of low-silica igneous rocks lies between the MORB and the volcanic arc array, indicating a weak subduction zone signal (Fig. 4a). The latter is compatible with geochemical features similar to those of calc-alkaline primitive arc magmas (Schmidt and Jagoutz, 2017, and references therein), as indicated for intrusions of the North Patagonian Andes yielding ages of ca. 330–323 Ma (Yoya et al., 2023). The dominance of depleted mantle sources is further supported by La/Yb *vs* Tb/Yb, La_N/Sm_N *vs* Tb_N/Yb_N and Gd_N/Yb_N *vs* La_N/Yb_N plots (Fig. 4b,c, d), which point to a depleted spinel peridotite with only very limited contribution of a more fertile, garnet-bearing source. In the northern PD, Devonian depleted spinel-bearing peridotites were reported by Plissart et al. (2019). The relatively low Nb/La values also reinforce this interpretation, whereas low Ba/Th contents mainly suggest slab-derived melts (Fig. 4e).

Both Dy/Yb and Nb/Ta *vs* SiO_2 plots reveal the dominance of amphibole fractionation in the source (Fig. 4f, g; Moyen, 2009; Li et al., 2017). Nevertheless, primitive arc compositions show a clear difference in the Eu/Eu* *vs* Sr/Y plot: Devonian intrusions exhibit negative Eu anomalies and low Sr/Y ratios, whereas Carboniferous-Permian plutons yield negligible to slightly positive Eu anomalies and higher Sr/Y values (Fig. 4h). This distinction highlights the role of plagioclase during crystal fractionation in Devonian plutons (Dessimoz et al., 2012). Early crystallization of plagioclase in the Devonian plutonic suite is further supported by the presence of plagioclase + amphibole cumulate rocks in the Pacific Domain (Rapela et al., 2021). Contrasting partition coefficients of Sr and Y in plagioclase and amphibole in hydrous mafic

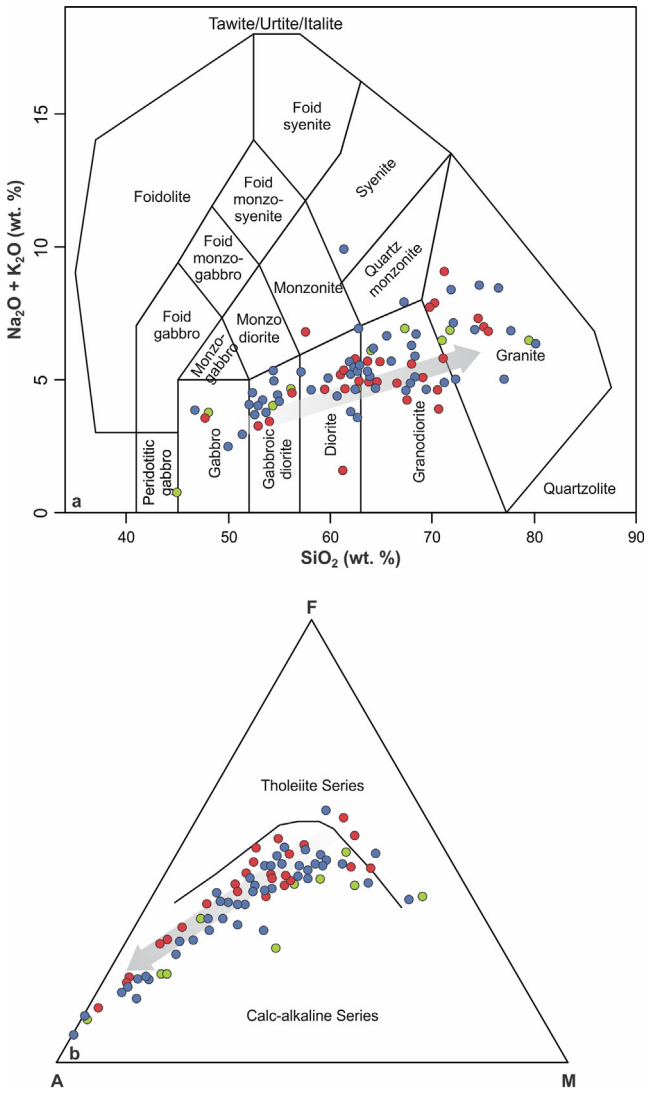

Fig. 2. TAS (a) and AFM (b) classification diagrams (Irvine and Baragar, 1971; Middlemost, 1994), showing that samples depict a typical calc-alkaline trend. Samples with a transitional tholeiitic to calc-alkaline signal correspond to primitive arc compositions. Green: Devonian rocks of the Pacific Domain (PD), red: Devonian rocks of the NPA and the NPM, blue: Carboniferous-Permian rocks of the NPA and the NPM. (For interpretation of the references to colour in this figure legend, the reader is referred to the web version of this article.)

melts explain the increasing Sr/Y ratio from the Devonian to the Carboniferous-Permian as the result of increasing proportion of amphibole over plagioclase fractionation as residual magmatic phases (Dessimoz et al., 2012; Nielsen et al., 2017; Shimizu et al., 2017).

On the other hand, the temporal variations of Sr/Y, La_N/Yb_N and Eu/Eu* (chondrite-normalized) constrained by U-Pb zircon data of plutonic rocks are used to evaluate the evolution of arc crustal thickness related to subduction zone dynamics (Fig. 5). Whole-rock Sm-Nd and zircon Lu-Hf isotopic data were also included in the analysis to filter the possible influence of metasedimentary wall rocks in the geochemical signal due to assimilation/anatexis (Fig. 6), as documented by field evidence, zircon xenocrysts and isotopic data (Supplementary Data, Table S2; Pankhurst et al., 2006; Hervé et al., 2016; Serra-Varela et al., 2021). The temporal evolution of both Sr/Y and La_N/Yb_N show an increase from the Devonian to the Permian, though this trend is particularly well-defined for the former (Fig. 5). In contrast, Eu/Eu* values are

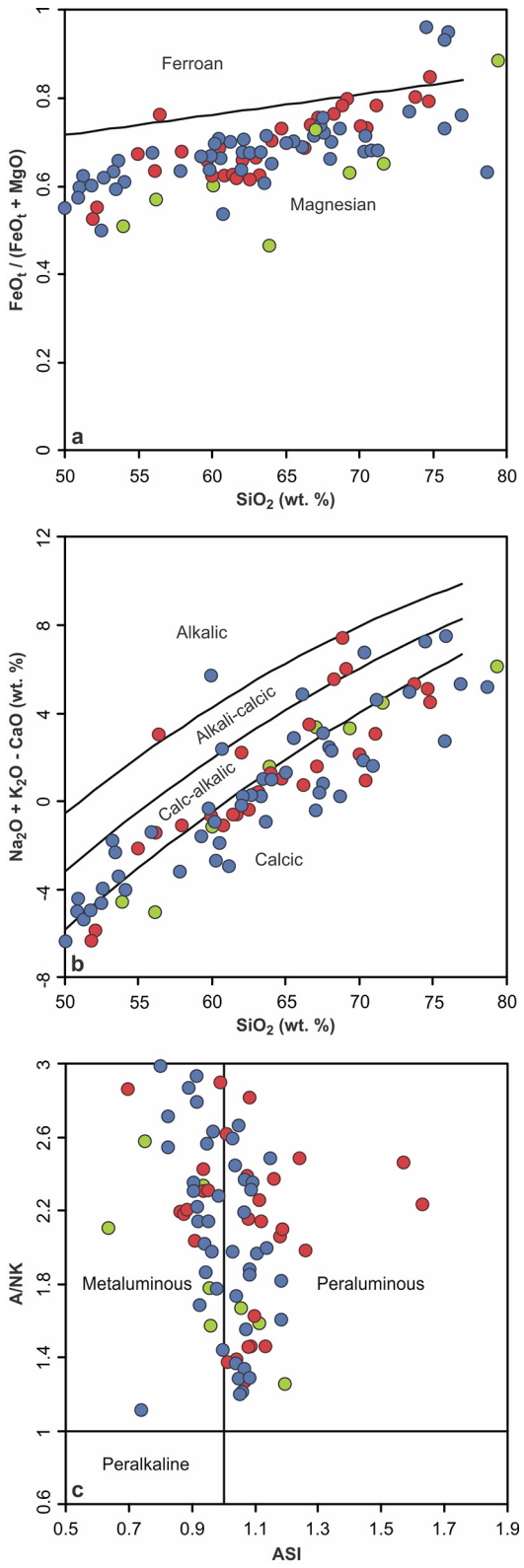

Fig. 3. Discrimination diagrams after Frost et al. (2001). The dominance of magnesian, calcic- to calc-alkalic, and meta- to peraluminous compositions point to a clear affinity with Cordilleran intrusions (Frost et al., 2001). Green: Devonian rocks of the PD, red: Devonian rocks of the NPA and the NPM, blue: Carboniferous-Permian rocks of the NPA and the NPM. (For interpretation of the references to colour in this figure legend, the reader is referred to the web version of this article.)

typically below 1, except for late Carboniferous intrusions, which yield negligible Eu anomalies.

Neither ε_{Nd} nor ε_{Hf} values correlate with Sr/Y (Fig. 6a, b), reflecting that crustal assimilation had a very subordinate influence on the Sr/Y ratios, which is further supported by the lack of correlation with A/CNK values (Fig. 7a). Likewise, Sr/Y of supracrustal rocks, represented by mean Upper Continental Crust (UCC) and Post-Archean Australian Shale (PAAS) compositions, are relatively low compared to most plutonic rocks, particularly those of late Carboniferous to Permian age. Therefore, Sr/Y seems to be a valid proxy documenting progressive late Carboniferous-Permian crustal thickening. The increase of Sr/Y may arise mainly from a progressive decrease in the proportion of plagioclase fractionation, which is dominant in the Devonian, and the relative increasing dominance of amphibole fractionation in the source (see also Fig. 5).

In contrast, La_N/Yb_N ratios are well-correlated with isotopic data, with higher La_N/Yb_N values associated with more negative subchondritic compositions (Fig. 6c, d). Furthermore, intrusions yielding relatively high La_N/Yb_N ratios show typical peraluminous compositions (Fig. 7b), indicating a correlation of La_N/Yb_N with crustal recycling processes. Since La_N/Yb_N of upper crustal rocks is typically low (Fig. 5b), the most likely explanation seems to be residual garnet fractionation. However, this process might not have taken place in the magmatic arc roots but, instead, at shallower depths during intracrustal differentiation, favored by aluminous crustal sources that allow garnet fractionation at relatively low pressures (Moyen, 2009). Consequently, the typical assumption of increasing magma source depth monitored by increasing La_N/Yb_N is not valid in this case.

In the case of Eu/Eu*, temporal variations exhibit a complex pattern. Devonian plutonic rocks typically have negative Eu anomalies and correlate with the Sr/Y ratio (Fig. 4h, 5c). Though no clear trend is observed when compared with isotopic data (possibly due to the low number of samples; Fig. 6e, f), Fig. 7c clearly demonstrates that these negative Eu anomalies occur in both meta- and peraluminous intrusions. On the other hand, a different situation is observed for the Gondwanide magmatism. Late Carboniferous intrusions yield the highest values (i.e., negligible to slightly positive Eu anomalies), whereas generally lower Eu/Eu* values characterize Permian rocks (Fig. 5c). Since negative Eu anomalies are typical of subchondritic and peraluminous compositions (Fig. 6e, 6f, 7c), Eu/Eu* ratios may reflect the incorporation of crustal material to some extent (e.g., Sawyer, 1998). Therefore, the Eu/Eu* fingerprint may result from a mixture of both source depth and upper crustal reworking.

Low Eu/Eu* values are present in all Devonian intrusions, independently of their meta- or peraluminous compositions (Fig. 7c), thus revealing plagioclase fractionation and shallow sources. This interpretation is supported by the presence of plagioclase-bearing cumulates that evidence early plagioclase crystallization in the PD (Fig. 8; Rapela et al., 2021). In contrast, Eu/Eu* values may only be representative of the source in the oldest Gondwanide plutons (ca. 330–320 Ma), nearly lacking in plagioclase fractionation. In contrast, Permian magmatic rocks show Eu/Eu* < 1 (i.e., negative Eu anomalies) that result mainly from crustal components, thus reaching Eu/Eu* compositions comparable to those of upper crustal rocks. Though crustal reworking seems to be a key process controlling Eu anomalies, it is also likely that plagioclase fractionation might have played a role.

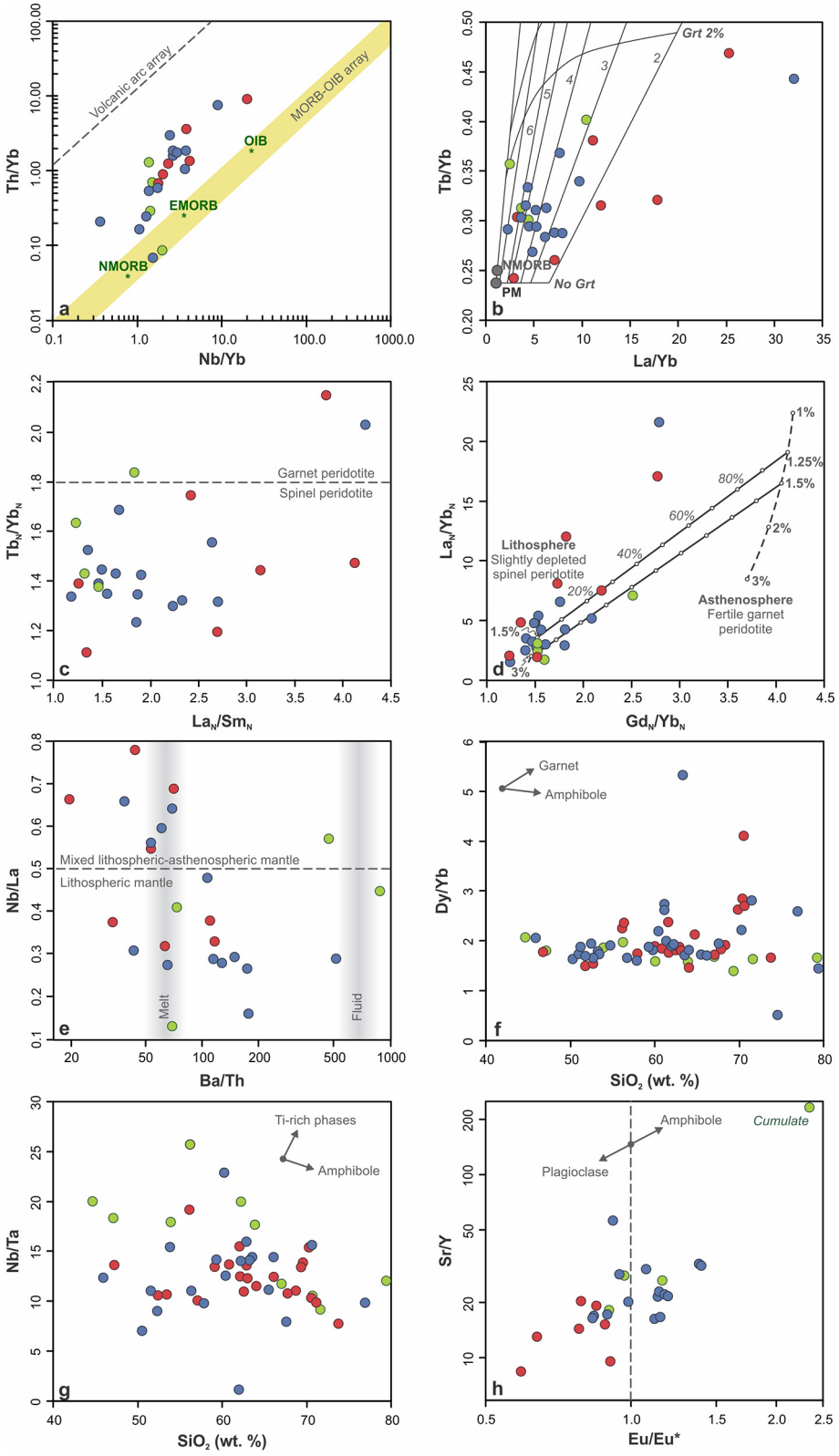

Fig. 4. Geochemical constraints on source characterization. Data in diagrams (a) to (e) and (h) correspond to primitive arc magma compositions (SiO_2 < 60 wt%). Normalization in (c) and (d) to primitive mantle (Sun and McDonough, 1989). (a) Nb/Yb vs Th/Yb (Pearce, 2008). (b) La/Yb vs Tb/Yb (George and Rogers, 2002). and (c) La_N/Sm_N vs Tb_N/Yb_N (Hou et al., 2015, and references therein). (d) Gd_N/Yb_N vs La_N/Yb_N (McGee et al., 2013).. (e) Ba/Th vs Nb/La. Ba/Th is used as a proxy of slab-derived melt and fluid components (Zamboni et al., 2016), whereas Nb/La is applied to discriminate between shallow and deep mantle sources (Abdel-Rahman and Nassar, 2004). (f) SiO_2 vs Dy/Yb (g) SiO_2 vs Nb/Ta. (h) Eu/Eu* vs Sr/Y. Results in (a) to (e) demonstrate the dominance of a shallow mantle source in the spinel stability field. On the other hand, diagrams (f) and (g) show dominance of amphibole fractionation, whereas (h) also highlights plagioclase fractionation in Devonian magmatism, which is nearly absent in younger units. Green: Devonian rocks of the PD, red: Devonian rocks of the NPA and the NPM, blue: Carboniferous-Permian rocks of the NPA and the NPM. (For interpretation of the references to colour in this figure legend, the reader is referred to the web version of this article.)

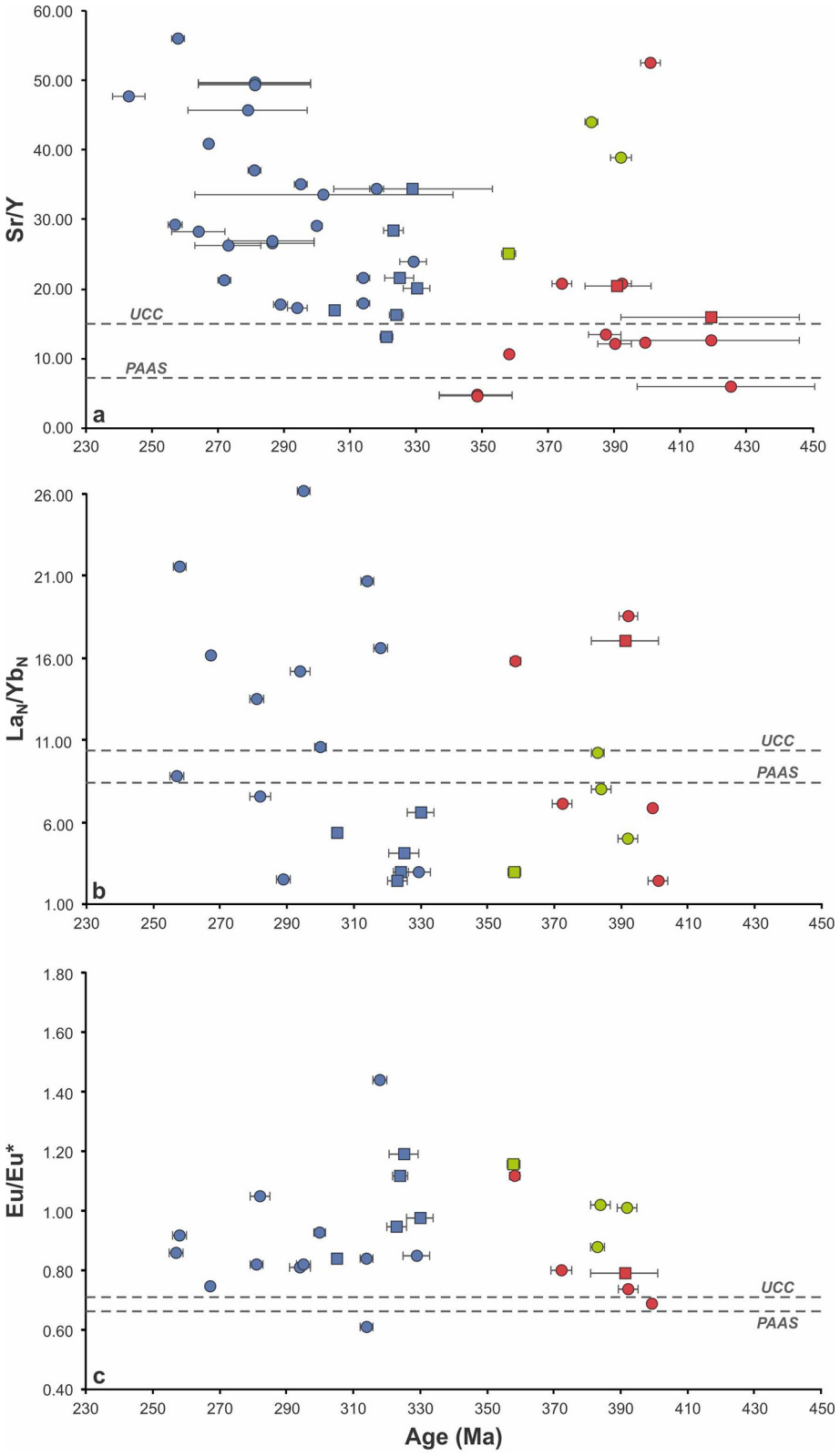

Fig. 5. Zircon U-Pb crystallization age vs geochemical proxies (squares: primitive arc compositions, SiO_2 < 60 wt%; circles: intermediate to felsic compositions, SiO_2 > 60 wt%). Sr/Y (a), La_N/Yb_N (b) and Eu/Eu* (c). Mean Upper Continental Crust (UCC) and Post-Archean Australian Shale (PAAS) compositions after McLennan (2001) and references therein. Green: Devonian rocks of the PD, red: Devonian rocks of the NPA and the NPM, blue: Carboniferous-Permian rocks of the NPA and the NPM. Sr/Y and, to a lesser extent, La_N/Yb_N, show an increase from the Devonian to the Permian. In contrast, Eu/Eu* values are typically below 1, except for late Carboniferous intrusions, which yield negligible Eu anomalies. See Figs. 6 and 7 for further details. (For interpretation of the references to colour in this figure legend, the reader is referred to the web version of this article.)

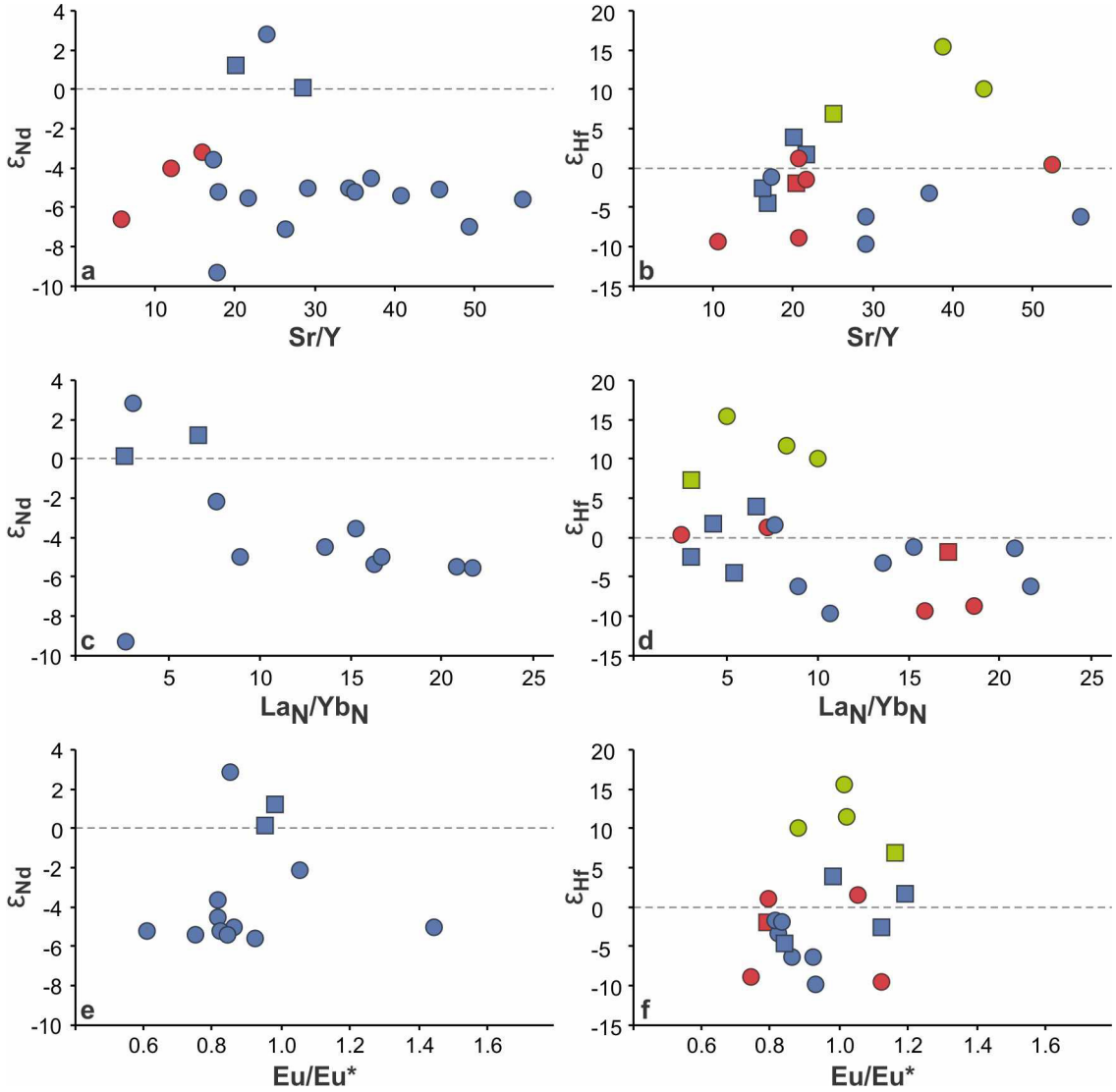

Fig. 6. Geochemical proxies *vs* whole-rock ε_{Nd} (a, c, e) and zircon ε_{Hf} (b, d, f) data. Dotted lines correspond to chondritic compositions. In the case of Lu-Hf isotopic data, ε_{Hf} correspond to the weighted average of the values obtained for individual zircons, recalculated to the reported concordia age. Green: Devonian rocks of the PD, red: Devonian rocks of the NPA and the NPM, blue: Carboniferous-Permian rocks of the NPA and the NPM. In the case of Sr/Y, no clear correlation with isotopic data is observed, whereas La_N/Yb_N shows a negative correlation with both ε_{Nd} and ε_{Hf}. Though no clear trend is observed for Eu/Eu* in Devonian rocks, Eu/Eu* values close to 1 are observed only for suprachondritic compositions of late Carboniferous to Permian rocks, whereas negative anomalies are mainly associated with subchondritic ε_{Nd} and ε_{Hf} values of the latter. (For interpretation of the references to colour in this figure legend, the reader is referred to the web version of this article.)

4.3. The U-Pb and Lu-Hf zircon archive of tectonomagmatic processes

Lu-Hf zircon data of magmatic plutons show a clear correlation with age, from variable subchondritic to suprachondritic ε_{Hf} between ca. −10 and + 15 in the Devonian to very negative values from ca. −5 to −15 in the late Permian (Fig. 9a). Devonian magmatism in the PD shows dominantly suprachondritic compositions that decrease to the late Devonian-Early Carboniferous. However, there is evidence of magmatism with a subchondritic fingerprint comparable to that recorded by coeval plutons in the NPA and the western NPM. After an early Carboniferous magmatic gap (Renda et al., 2021), well-documented by compiled U-Pb zircon data of Devonian to Permian magmatism in the study area (Fig. 9b) and also by detrital zircon data (e.g., Kirsch et al., 2016), late Carboniferous magmatism records slightly suprachondritic to slightly subchondritic ε_{Hf} values. This composition is not restricted to rocks of the NPA and the NPM, but is also shared by the Coastal Batholith in the northern segment of the Pacific Domain (Fig. 1; Deckart et al., 2014). To the late Permian, a progressively increasing subchondritic fingerprint is observed (Fig. 9a).

The widespread occurrence of suprachondritic magmas in the Devonian indicates a significant addition of juvenile mantle-derived crust (Hervé et al., 2016; Rapela et al., 2021). However, this process is related to local assimilation and anatexis, particularly in the magmatic arc exposures of the NPA and NPM (Fig. 1), which result in subchondritic compositions. In contrast, the negative trend depicted by late Carboniferous to Permian intrusions, even in the Pacific Domain, is mainly related to increasing crustal components due to enhanced crustal reworking, also supported by the temporal variation of La_N/Yb_N and Eu/Eu* ratios (Fig. 6). Nevertheless, the primary source of Gondwanide magmatism seems to be a MORB-like source, as indicated by geochemical data and isotopic compositions of the primitive arc melts, mainly of late Carboniferous age (Figs. 5, 9).

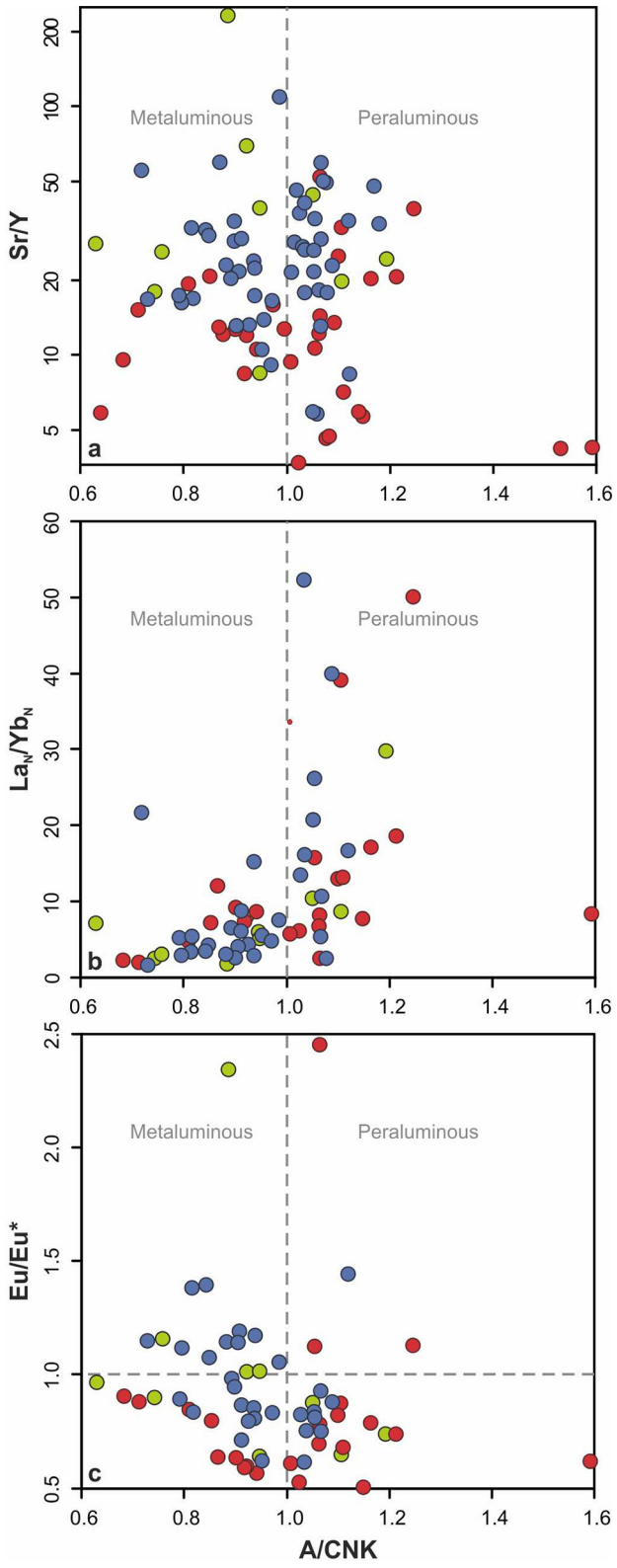

Fig. 7. Alumina saturation index (ACN/K) *vs* Sr/Y (a), La_N/Yb_N (b), and Eu/Eu* (c). Green: Devonian rocks of the PD, red: Devonian rocks of the NPA and the NPM, blue: Carboniferous-Permian rocks of the NPA and the NPM. Sr/Y shows no correlation with the alumina saturation index, whereas a positive correlation is observed for La_N/Yb_N. On the other hand, Devonian rocks of the PD, NPA and NPM show a dominance of negative Eu anomalies for both meta- and peraluminous compositions, whereas a negative correlation between Eu/Eu* and ACN/K is evident for late Carboniferous to Permian intrusions. (For interpretation of the references to colour in this figure legend, the reader is referred to the web version of this article.)

5. Discussion

5.1. Paleozoic accretionary orogens: The growth and stabilization of Patagonia

Dynamics of convergent margins and resulting accretionary orogens are primary controls on tectonomagmatic processes occurring in associated arc magmas, being particularly relevant for source depth and subsequent intracrustal differentiation mechanisms. However, arc dynamics and alternating periods of magmatic flare-ups and lulls are not solely influenced by external drivers such as large-scale tectonics but also by internal cyclic processes (e.g., Ducea et al., 2015; Kirsch et al., 2016; Chapman et al., 2017, 2021).

In the case of Patagonia, the geochemical fingerprint of Devonian and late Carboniferous-Permian intrusions shows no major differences in terms of their dominant mantle source (Fig. 4a to e). Therefore, most differences seem to be related to intracrustal fractionation processes (Fig. 4f to h; Section 4), which are likely to be related to regional tectonic controls (see below).

5.1.1. Devonian arc dynamics and slab roll-back

The evolution of Devonian magmatism was mainly controlled by plagioclase + amphibole fractionation in the source, as documented by relics of cumulates (Fig. 8; Rapela et al., 2021). This evidence is in line with low Sr/Y values and negative Eu anomalies of intrusions (Section 4.2), which in turn indicate shallow sources and, therefore, a relatively thin crust (e.g., Chapman et al., 2015; Chiaradia, 2015; Ducea et al., 2015; Profeta et al., 2015). This is further supported by the common occurrence of juvenile magmas, which are particularly well-recorded in the PD by suprachondritic isotopic compositions of arc intrusions (e.g., Fig. 9a) and are also associated with metamafic and metaultramafic rocks, including pillow metabasalts (Fig. 1; Hervé et al., 2016; Plissart et al., 2019; Rapela et al., 2021). In addition, a thin continental crust is supported by high geothermal gradients documented by Devonian regional metamorphism in the NPA, associated with low-pressure (<ca. 4–5 kbar) medium- to high-grade conditions (Martínez et al., 2012; Serra-Varela et al., 2019).

Retreating accretionary orogens are the common locus of juvenile arc magmatism, since they are associated with crustal extension/transtension that favors crustal thinning and mantle-derived magma emplacement in the forearc to the back-arc regions (Collins, 2002; Kemp et al., 2009; Ducea et al., 2015). Such a setting could explain the dominance of shallow magmatic sources for Devonian magmatism and the prevailing juvenile magmatism, possibly as the result of slab roll-back (Fig. 10a, b; Rapela et al., 2021). The trenchward migration of the arc, linked to a retreating accretionary orogen, is in line with the presence of Ordovician arc relics at the northeastern NPM (e.g., Pankhurst et al., 2014; González et al., 2021). The evidence of arc-related Silurian anatexis at ca. 434 Ma in the NPA (Serra-Varela et al., 2019), spatially associated with Devonian intrusions, may suggest a Silurian onset of subduction in the region.

Previous proposals have postulated the existence of an island arc in the PD, i.e. Chaitenia, which was accreted by the late Devonian-early Carboniferous to a continental magmatic arc, represented by intrusions located in the NPA and the western NPM that yield subchondritic Lu-Hf compositions (Hervé et al., 2016, 2018; Rapela et al., 2021). Nevertheless, the wall rock of PD Devonian intrusions corresponds to metasedimentary sequences derived from the continental margin (Hervé et al., 2018), implying that both arc segments were relatively close to each other. The existence of two adjacent subduction zones is thus highly unlikely. Furthermore, felsic metaigneous rocks with subchondritic Lu-Hf

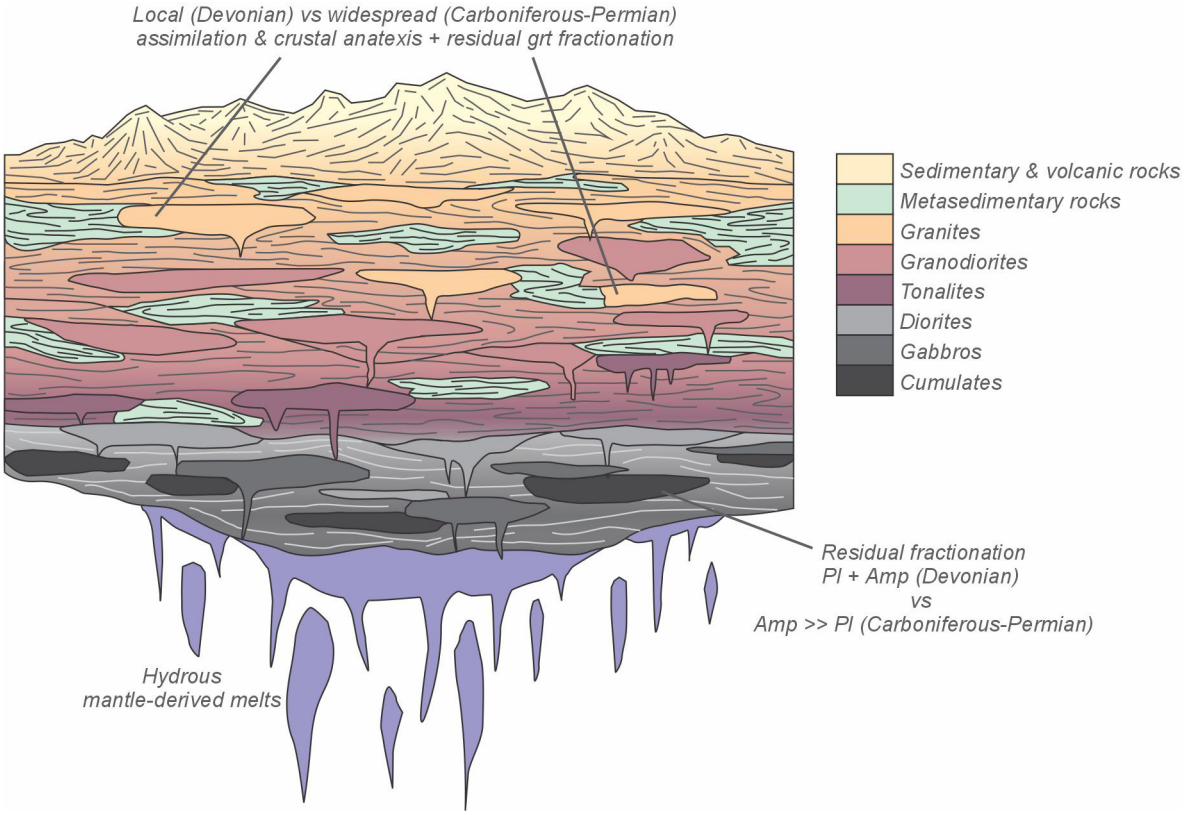

Fig. 8. Schematic magmatic arc section, showing main petrogenetic differences between the Devonian and late Carboniferous-Permian magmatism.

isotopic fingerprint evidence the presence of continental crust in the PD (Fig. 9a; Hervé et al., 2016; Rapela et al., 2021). Instead of an island arc complex in the Pacific Domain, evidence points to a simpler, yet more plausible mechanism of *in situ* juvenile addition. The PD may thus represent relics of oceanic rocks and forearc magmatism. The dominance of suprachondritic Lu-Hf compositions, in contrast to characteristic subchondritic values of intrusions located to the east, might thus be the result of a progressively thinner Paleozoic metasedimentary pile towards the forearc (e.g., Chapman et al., 2017). More significant assimilation and/or anatexis in the main arc domain (Rapela et al., 2021; Serra-Varela et al., 2021) may explain the local presence of subchondritic magmas.

5.1.2. Early Carboniferous magmatic lull

The magmatic lull at ca. 350–330 Ma is well-documented by igneous and detrital zircon U-Pb data (Fig. 8b; Kirsch et al., 2016; Renda et al., 2021). Within this period, only one intrusion was dated at 348 ± 11 Ma at the northwesternmost NPM (U-Pb TIMS; Varela et al., 2005), whereas no record of metamorphism has been reported so far. The general decrease in the ε_{Hf} values of Devonian intrusions towards the Devonian-Carboniferous boundary suggests a tectonometamorphic event (Rapela et al., 2021; Renda et al., 2021), possibly related to a short-lived compressional/transpressional pulse after protracted extension-related subduction. Rapela et al. (2021) attributed this episode to the island arc collision, though this hypothesis seems unlikely (see Section 5.1.1). Alternatively, a non-collisional mechanism linked to changing conditions in the subduction zone may explain the observed magmatic lull (e.g., Kirsch et al., 2016; Chapman et al., 2021).

Since no significant changes are observed in the mantle source for magmatism pre- and post-dating the lull, mechanisms involving generation of slab windows and ascent of deep asthenospheric mantle sources (e.g., Kirsch et al., 2016, Chapman et al., 2021) cannot be invoked. An alternative model considers subduction of a dry lithospheric mantle linked to incorporation of hyperextended continental slivers in the subduction channel, as suggested for the pre-collisional history of Alps (McCarthy et al., 2021, and references therein). This mechanism might have played a role, considering partial subduction of the previously extended Devonian forearc basins during a late Devonian transpressional/compressional event (Plissart et al., 2019; Rapela et al., 2021; Renda et al., 2021). However, the existence of a widespread Devonian magmatic arc marks a significant difference with the Alpine case, since the dominance of a hydrous mantle (e.g., Section 4.2, Fig. 9.1) contrasts significantly with the anhydrous source of rift-related pre-collisional Alpine basins.

On the other hand, paleogeographic reconstructions show a significant change in global convergence parameters at ca. 350–340 Ma (Young et al., 2019). For the Patagonian region, this transition implies a change from Devonian trenchward to late Carboniferous inland migration of the subduction zone (Young et al., 2019), which is compatible with the proposed tectonic model from retreating to advancing accretionary orogens (Fig. 10). Slow oblique subduction leading to strike-slip-dominated deformation along the proto-Pacific margin might have been likely during this transitional stage and may explain the absence of arc magmatism, also invoked to explain the lack of arc-related magmatism in the Alps (e.g., Zanchetta et al., 2012). This process, intimately related to a major plate reorganization due to the onset of convergence leading to the final assembly of Pangea, culminates with the Gondwanide Orogeny in the study area (Section 5.1.3; Oriolo et al., 2019).

In summary, the combination of both large-scale geodynamic and arc-related intrinsic processes might have triggered the magmatic lull. A transient geodynamic context seems to have played a major role, being possibly linked to the development of a rela-

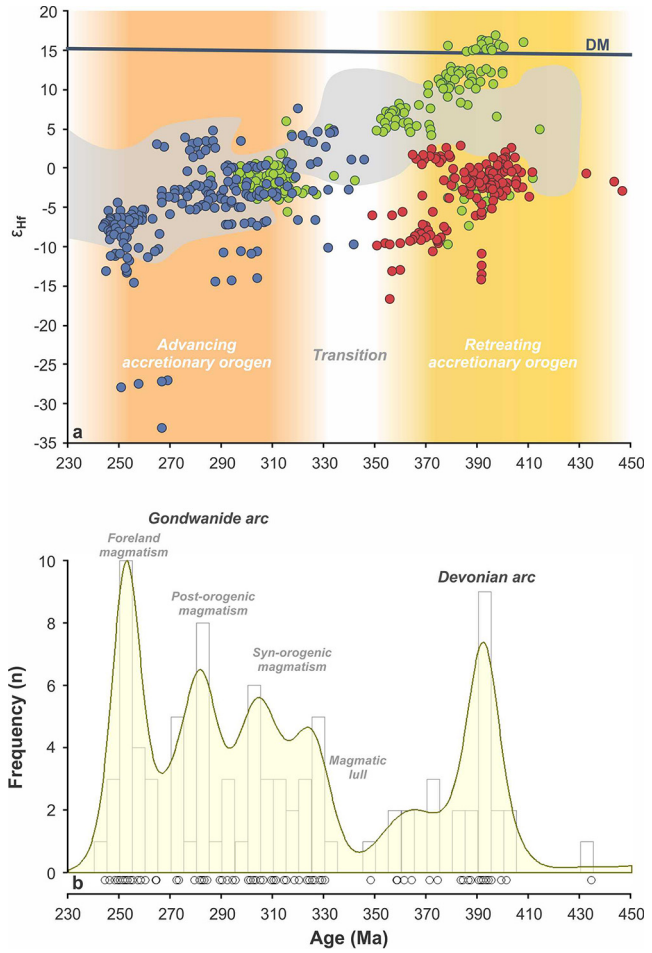

Fig. 9. (a) Zircon U-Pb crystallization age vs ε_{Hf} (Supplementary Data 1, Supplementary Table 2). The grey area shows the isotopic trend of the Antarctic Peninsula and Thurston Island (Nelson and Cottle, 2018, and references therein). All data recalculated using parameters of Supplementary Table 2. PD data also include Carboniferous intrusions of the Coastal Batholith (Deckart et al., 2014). (b) Kernel density estimate curves and histograms plotted using DensityPlotter (Vermeesch, 2012) for zircon U-Pb data of magmatic rocks of Patagonia (n = 89; see references in Supplementary Data 1). Bin and band width = 5 My. DM: depleted mantle.

tively short-lived transcurrent margin with slow convergence rates. However, further evidence is required to properly understand the tectonic significance of this gap.

5.1.3. Late Carboniferous to Permian arc dynamics and the Gondwanide Orogeny

Voluminous late Carboniferous to Permian magmatism is associated with a magmatic flare-up linked to the transpressional Gondwanide orogeny, a widespread tectonometamorphic event in northern Patagonia (Fig. 9b, 10c, 10d; Martin et al., 1999; Oriolo et al., 2019). Thermobarometric data of metasedimentary rocks show regional high-temperature and medium- to high-pressure conditions for late Carboniferous to early Permian metamorphism and deformation in the NPA and the western NPM, pointing to significant crustal shortening and thickening (Marcos et al., 2020; Oriolo et al., 2019; Renda et al., 2021; von Gosen, 2009).

The protracted duration of the Gondwanide magmatism resulted from the spatio-temporal variations of the arc (Fig. 10d). After the magmatic lull, magmatism resumed at ca. 330–320 Ma, with emplacement of relatively juvenile, primitive arc magmas at the NPA and the western NPM (Fig. 8). The primitive arc signature of Gondwanide magmatism is restricted to these early pulses related to the onset of subduction (Yoya et al., 2023), whereas younger intrusions are generally more evolved and show a more significant crustal component, which is ubiquitous from the Pacific Domain to the western North Patagonian Massif, suggesting a common evolution along the ca. NNW-SSE-striking magmatic arc (Renda et al., 2019, and references therein). These early intrusions show a contrasting, amphibole-dominated deeper source than comparable Devonian primitive intrusions, which are characterized by plagioclase and amphibole fractionation (Fig. 4h, 5a; Rapela et al., 2021; Yoya et al., 2023).

In general, late Carboniferous magmatism is synorogenic, as documented by structural evidence, and is followed by early to middle Permian post-orogenic magmatism (Pankhurst et al., 2006; Renda et al., 2019, 2021). By the middle to late Permian, the magmatic and deformation front migrated further east, reaching the foreland region in the central and eastern NPM, and the Ventania System (Figs. 1, 9b, 10d; von Gosen, 2003; Pankhurst et al., 2006; Martínez Dopico et al., 2017; Gregori et al., 2020; Renda, 2020; Ballivián Justiniano et al., 2023). In particular, deformation and magmatism are well-constrained at ca. 260–250 Ma at the northeastern NPM (Martínez-Dopico et al., 2017, and references therein).

Crustal shortening and thickening driven by progressive transpression (Oriolo et al., 2019; Marcos et al., 2020; Renda et al., 2021) favored increasing depths of magma source (i.e., fractionation of amphibole ≫ plagioclase) and increasing crustal reworking documented by Lu-Hf isotopic data, and La_N/Yb_N and Eu/Eu* temporal variations (Figs. 5, 8). A comparable trend is revealed by decreasing Th/U ratios in late Carboniferous to Permian magmatic zircons (Renda et al., 2021). Likewise, the shift towards highly subchondritic ε_{Hf} values of late Permian foreland magmatism (Fig. 9) can be explained by the existence of a relatively thicker and maybe older crust than in western domains (e.g., Chapman et al., 2017), as the result of the previous late Cambrian to Ordovician tectonometamorphic event in the northeastern NPM (González et al., 2021, and references therein).

The development of an advancing accretionary orogeny during Gondwanide transpressional deformation and crustal thickening is further supported by paleogeographic reconstructions (Oriolo et al., 2019; Young et al., 2019), indicating an inland migration of the paleo-Pacific trench. This reconstruction also reinforces the relationship between the Gondwanide Orogeny with the global plate reorganization during the Pangea assembly (Oriolo et al., 2019), as proposed in other peripheral regions of Gondwana (Cawood et al., 2021). On the other hand, the documented migration pattern of deformation and magmatism points to slab shallowing as the most likely trigger, favoring increasing interplate coupling and thus crustal shortening (e.g., Cawood et al., 2009). By the Permian-Triassic transition, slab break-off led to the final collapse of the Gondwanide Orogen and the flare-up documented in northeastern Patagonia (Fig. 9b; Gianni and Navarrete, 2022; Falco et al., 2022).

5.2. The roots of Patagonia

Collisional models of Patagonia have classically assumed that crustal domains such as the North Patagonian and Deseado Massifs behaved as wandering continents during the Paleozoic, thus implying the existence of Precambrian basement rocks and a relatively thick continental crust. Though several contributions have suggested the existence of possible Mesoproterozoic lower crustal roots in Patagonia (e.g., Rapela and Pankhurst, 2020; Rapela et al., 2021), no Precambrian rocks have been identified so far. The zircon record of Patagonia and the Malvinas/Falkland Plateau points to a juvenile late Mesoproterozoic source, possibly corre-

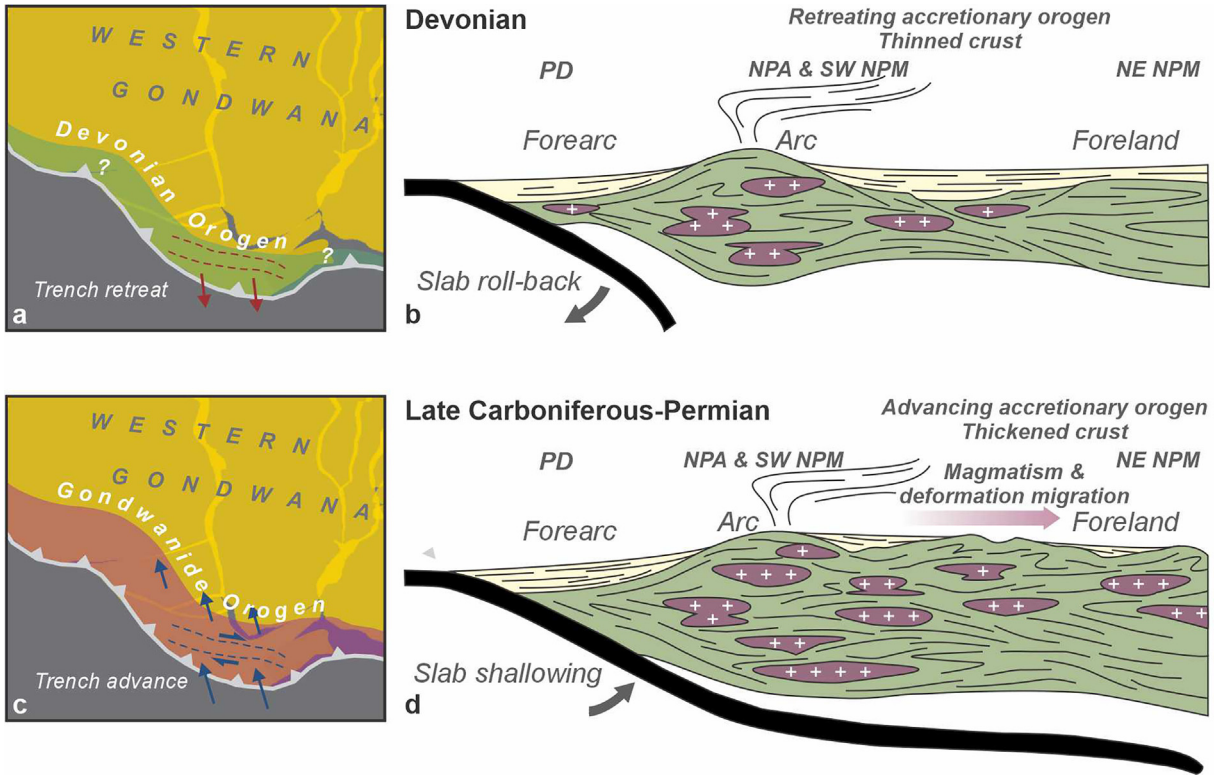

Fig. 10. Schematic paleogeographic reconstructions (a, c) and tectonic setting (b, d), with simplified convergence parameters after Vizán et al. (2017) and Young et al. (2019). Dotted lines show the schematic position of the Devonian (red) and Carboniferous-early Permian (blue) arcs depicted in Fig. 1. (a, b) Devonian retreating accretionary orogen and resulting thinned crust. (c, d) Late Carboniferous to Permian advancing accretionary orogen related to dextral transpression and resulting thickened crust. The presence of middle to late Permian magmatism in the eastern North Patagonian Massif resulted from inland migration due to slab shallowing. PD: Pacific Domain, NPA: North Patagonian Andes, SW & NE NPM: southwestern & northeastern North Patagonian Massif. (For interpretation of the references to colour in this figure legend, the reader is referred to the web version of this article.)

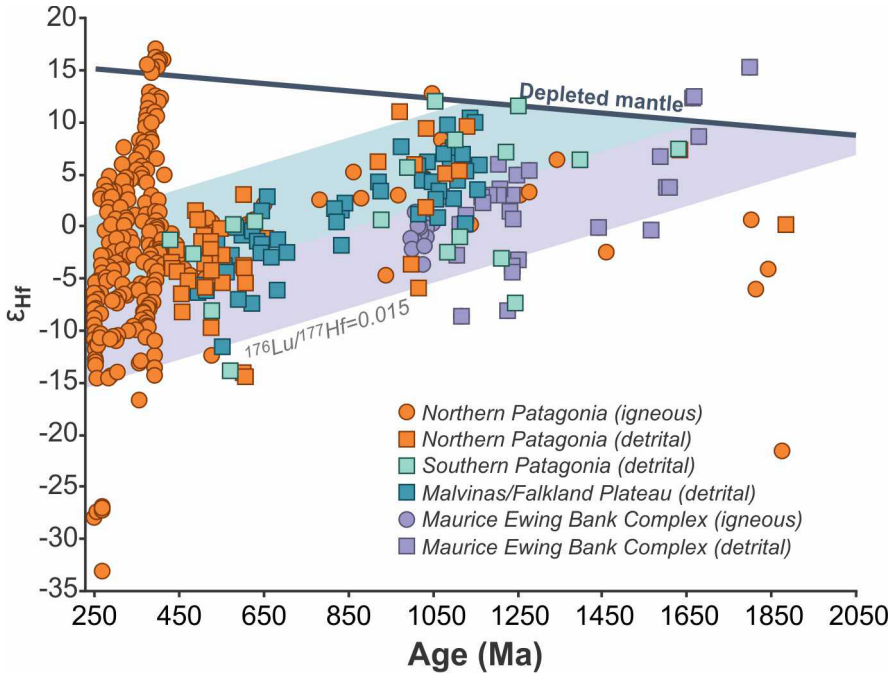

Fig. 11. Lu-Hf zircon isotopic data of Paleozoic magmatic and metasedimentary rocks of northern Patagonia, late Paleozoic metasedimentary rocks of southern Patagonia, Paleozoic sedimentary rocks of the Malvinas/Falkland Plateau and Mesoproterozoic basement rocks of the Maurice Ewing Bank in the South Atlantic Offshore (see references in Supplementary Data 1; Augustsson et al., 2006; Ramos et al., 2017; Chemale et al., 2018). All data recalculated using parameters of Supplementary Table 2. The zircon record of Patagonia suggests reworking of a juvenile late Mesoproterozoic source, possibly corresponding to the Mesoproterozoic basement of the Malvinas/Falkland Plateau, though rocks such as those of the Maurice Ewing Bank might also have contributed to some extent. Nevertheless, even if such Mesoproterozoic relics were present in the Patagonian basement, they were significantly reworked during Paleozoic orogenic events, which also contributed to crustal addition.

sponding to Mesoproterozoic basement rocks of the latter (Ramos et al., 2017). Despite basement rocks of the Maurice Ewing Bank show a slightly more subchondritic trend (Chemale et al., 2018), they might have contributed to some extent as well (Fig. 11). Nevertheless, Lu-Hf isotopic trends demonstrate that, even if Mesoproterozoic relics were present in the Patagonian crust, they were significantly reworked during Paleozoic orogenic events (Fig. 11). This is particularly well-documented by Precambrian to early Paleozoic zircon xenocrysts in Paleozoic intrusions that are comparable to detrital zircons of Paleozoic metasedimentary sequences (e.g., Pankhurst et al., 2006), which are ubiquitous in the Patagonian basement. Reworked, mainly metasedimentary continental crust was thus mixed with juvenile mantle-derived magmas during Paleozoic arc magmatism, which contributed to addition of juvenile crust to some extent. Consequently, Paleozoic accretionary orogens played a major role in the generation of the continental crust of Patagonia, implying protracted recycling of (meta)sedimentary sequences, crustal reworking due to assimilation and anatexis, and juvenile magma addition. The Gondwanide Orogeny was particularly crucial for maturing and stabilizing the continental margin, since widespread crustal thickening resulting from transpression and magmatic addition favored the maturation and subsequent relative stabilization of an otherwise thin crust (Oriolo et al., 2019).

The proposed model of *in situ* Paleozoic growth of Patagonia is also reinforced by well-established correlations with southern Patagonia and the Antarctic Peninsula, and a common tectonomagmatic evolution during the Paleozoic (Bastias et al., 2020, and references therein), as shown by similarities in the Lu-Hf isotopic record as well (Fig. 9a; Nelson and Cottle, 2018, and references therein). Several Triassic to Jurassic accretionary complexes are documented in southwestern Patagonia (e.g., Hervé et al., 2008; Suárez et al., 2019) and indicate a protracted Paleozoic to Mesozoic accretionary growth towards the southwest (present coordinates). Likewise, a comparable *in situ* Paleozoic crustal growth model related to Paleozoic accretionary orogens was proposed for the Antarctic Peninsula (Burton-Johnson and Riley, 2015), being thus also compatible with accretionary processes documented further north (Capaldi et al., 2021, and references therein).

6. Conclusions

Late Paleozoic dynamics of accretionary orogens in northern Patagonia are intimately linked with tectonomagmatic processes that evolved significantly between the Devonian and the Carboniferous-Permian. Thus, the genesis of the continental crust of Patagonia is largely dominated by *in situ* crustal growth mechanisms related to Paleozoic accretionary orogens, challenging classical collisional models for the region. The Devonian arc evolved as part of a retreating accretionary orogen, leading to crustal extension/transtension and a relatively thin crust that favored widespread emplacement of juvenile magmas derived from shallow sources. In contrast, the late Carboniferous-Permian Gondwanide Orogeny was related to transpressional deformation, and crustal shortening and thickening, which forced a progressively deepening of primary magma sources and increasing contribution of crustal sources. Widespread magmatism and crustal thickening during this flare-up magmatic event resulted in a relative maturation and subsequent stabilization of the Patagonian continental crust.

CRediT authorship contribution statement

Sebastián Oriolo: Conceptualization, Data curation, Funding acquisition, Visualization, Writing – original draft. **Pablo D. González:** Conceptualization, Data curation, Funding acquisition, Writing – review & editing. **Emiliano M. Renda:** Data curation, Visualization, Writing – review & editing. **Miguel A.S. Basei:** Data curation, Writing – review & editing. **Juan Otamendi:** Data curation, Writing – review & editing. **Pablo Cordenons:** Data curation, Writing – review & editing. **Paulo Marcos:** Data curation, Writing – review & editing. **María Belén Yoya:** Writing – review & editing. **Carlos A. Ballivián Justiniano:** Writing – review & editing. **Rodrigo Suárez:** Writing – review & editing.

Declaration of Competing Interest

The authors declare that they have no known competing financial interests or personal relationships that could have appeared to influence the work reported in this paper.

Acknowledgements

Sebastián Oriolo thanks financial support of the National Geographic Society (grant CP-123R-17), Agencia Nacional de Promoción Científica y Tecnológica (PICT-2017-1092) and CONICET (PIP 11220200101662CO).

Appendix A. Supplementary material

Supplementary data to this article can be found online at https://doi.org/10.1016/j.gr.2023.05.011.

References

Abdel-Rahman, A.F.M., Nassar, P.E., 2004. Cenozoic volcanism in the Middle East: petrogenesis of alkali basalts from northern Lebanon. Geol. Mag. 141 (5), 545–563.

Augustsson, C., Mu̇nker, C., Bahlburg, H., Fanning, C.M., 2006. Provenance of late Palaeozoic metasediments of the SW South American Gondwana margin: a combined U-Pb and Hf-isotope study of single detrital zircons. J. Geol. Soc. 163 (6), 983–995.

Ballivián Justiniano, C.A., Oriolo, S., Basei, M.A.S., Lanfranchini, M.E., Christiansen, R. O., Uriz, N.J., Vázquez Lucero, S.E., Del Bono, D.A., Forster, M.A., Etcheverry, R.O., Tassinari, C.C.G., Comerio, M.A., Prezzi, C.B., 2023. The Gondwanide deformation along the southwestern border of the Río de la Plata Craton: Geochemical and geochronological constraints on ductile shear zones from the Ventania System basement, Argentina. J. S. Am. Earth Sci. 124, 104275.

Bastias, J., Spikings, R., Ulianov, A., Riley, T., Burton-Johnson, A., Chiaradia, M., Baumgartner, L., Hervé, F., Bouvier, A.-S., 2020. The Gondwanan margin in West Antarctica: insights from Late Triassic magmatism of the Antarctic Peninsula. Gondwana Res. 81, 1–20.

Burton-Johnson, A., Riley, T.R., 2015. Autochthonous v. accreted terrane development of continental margins: a revised in situ tectonic history of the Antarctic Peninsula. J. Geol. Soc. 172 (6), 822–835.

Capaldi, T.N., McKenzie, N.R., Horton, B.K., Mackaman-Lofland, C., Colleps, C.L., Stockli, D.F., 2021. The detrital zircon record of Phanerozoic magmatism in the southern central Andes. Geosphere 17, 876–897.

Cawood, P.A., Kröner, A., Collins, W.J., Kusky, T.M., Mooney, W.D., Windley, B.F., 2009. Accretionary orogens through Earth history. Geol. Soc. Spec. Pub. 318 (1), 1–36.

Cawood, P.A., Martin, E.L., Murphy, J.B., Pisarevsky, S.A., 2021. Gondwana's interlinked peripheral orogens. Earth Planet. Sci. Lett. 568, 117057.

Chapman, J.B., Ducea, M.N., DeCelles, P.G., Profeta, L., 2015. Tracking changes in crustal thickness during orogenic evolution with Sr/Y: An example from the North American Cordillera. Geology 43 (10), 919–922.

Chapman, J.B., Ducea, M.N., Kapp, P., Gehrels, G.E., DeCelles, P.G., 2017. Spatial and temporal radiogenic isotopic trends of magmatism in Cordilleran orogens. Gondwana Res 48, 189–204.

Chapman, J.B., Shields, J.E., Ducea, M.N., Paterson, S.R., Attia, S., Ardill, K.E., 2021. The causes of continental arc flare ups and drivers of episodic magmatic activity in Cordilleran orogenic systems. Lithos 398, 106307.

Chemale Jr, F., Ramos, V.A., Naipauer, M., Girelli, T.J., Vargas, M., 2018. Age of basement rocks from the Maurice Ewing Bank and the Falkland/Malvinas Plateau. Precambrian Res. 314, 28–40.

Chernicoff, C.J., Zappettini, E.O., Santos, J.O.S., McNaughton, N.J., Belousova, E., 2013. Combined U-Pb SHRIMP and Hf isotope study of the Late Paleozoic Yaminué Complex, Río Negro province, Argentina: Implications for the origin and evolution of the Patagonia composite terrane. Geosci. Frontiers 4, 37–56.

Chiaradia, M., 2015. Crustal thickness control on Sr/Y signatures of recent arc magmas: an Earth scale perspective. Sci. Rep. 5, 1–5.

Collins, W.J., 2002. Nature of extensional accretionary orogens. Tectonics 21 (4), 6-1–6-12.

Collins, W.J., Belousova, E.A., Kemp, A.I.S., Murphy, J.B., 2011. Two contrasting Phanerozoic orogenic systems revealed by hafnium isotope data. Nat. Geosci. 4 (5), 333–337.
Condie, K.C., 2007. Accretionary orogens in space and time. Geol. Soc. Am. Mem. 200, 145–158.
Deckart, K., Hervé Allamand, F., Fanning, M., Ramírez, V., Calderón, M., Godoy, E., 2014. U-Pb geochronology and Hf-O isotopes of zircons from the Pennsylvanian Coastal Batholith, south-central Chile. Andean Geol. 41, 49–82.
Dessimoz, M., Müntener, O., Ulmer, P., 2012. A case for hornblende dominated fractionation of arc magmas: the Chelan Complex (Washington Cascades). Contrib. Mineral. Petrol. 163 (4), 567–589.
Ducea, M.N., Saleeby, J.B., Bergantz, G., 2015. The architecture, chemistry, and evolution of continental magmatic arcs. Ann. Rev. Earth Planet. Sci. 43 (1), 299–331.
Falco, J.I., Hauser, N., Scivetti, N., Reimold, W.U., Folguera, A., 2022. The origin of Patagonia: insights from Permian to Middle Triassic magmatism of the North Patagonian Massif. Geol. Mag. 159 (9), 1490–1512.
Forsythe, R., 1982. The late Palaeozoic to early Mesozoic evolution of southern South America: a plate tectonic interpretation. J. Geol. Soc. 139 (6), 671–682.
Franzese, J.R., 1995. El Complejo Piedra Santa (Neuquén, Argentina): parte de un cinturón metamórfico neopaleozoico del Gondwana suroccidental. Andean Geol. 22, 193–202.
Frost, B.R., Barnes, C.G., Collins, W.J., Arculus, R.J., Ellis, D.J., Frost, C.D., 2001. A geochemical classification for granitic rocks. J. Petrol. 42, 2033–2048.
Gaetani, G.A., Kent, A.J., Grove, T.L., Hutcheon, I.D., Stolper, E.M., 2003. Mineral/melt partitioning of trace elements during hydrous peridotite partial melting. Contrib. Mineral. Petrol. 145, 391–405.
George, R., Rogers, N., 2002. Plume dynamics beneath the African plate inferred from the geochemistry of the Tertiary basalts of southern Ethiopia. Contrib. Mineral. Petrol. 144 (3), 286–304.
Gianni, G.M., Navarrete, C.R., 2022. Catastrophic slab loss in southwestern Pangea preserved in the mantle and igneous record. Nature Comm. 13, 1–15.
González, P.D., Sato, A.M., Naipauer, M., Varela, R., Basei, M., Sato, K., Llambías, E.J., Chemale, F., Castro Dorado, A., 2018. Patagonia-Antarctica Early Paleozoic conjugate margins: Cambrian synsedimentary silicic magmatism, U-Pb dating of K-bentonites, and related volcanogenic rocks. Gondwana Res. 63, 186–225.
González, P.D., Naipauer, M., Sato, A.M., Varela, R., Basei, M.A.S., Cábana, M.C., Vlach, S.R.F., Arce, M., Parada, M., 2021. Early Paleozoic structural and metamorphic evolution of the Transpatagonian Orogen related to Gondwana assembly. Int. J. Earth Sci. 110 (1), 81–111.
Gregori, D.A., Strazzere, L., Barros, M., Benedini, L., Marcos, P., Kostadinoff, J., 2020. The Mencué batholith: Permian episodic arc-related magmatism in the western North Patagonian Massif, Argentina. Int. Geol. Rev. 63, 317–341.
Gregori, D.A., Strazzere, L., Barros, M., Benedini, L., Marcos, P., Kostadinoff, J., 2021. The Mencué batholith: Permian episodic arc-related magmatism in the western North Patagonian Massif, Argentina. Int. Geol. Rev. 63 (3), 317–341.
Haschke, M., Gunther, A., 2003. Balancing crustal thickening in arcs by tectonic vs. magmatic means. Geology 31, 933–936.
Heredia, N., García-Sansegundo, J., Gallastegui, G., Farias, P., Giacosa, R., Alonso, J.L., Busquets, P., Charrier, R., Clariana, P., Colombo, F., Cuesta, A., Gallastegui, J., Giambiagi, L., González-Menéndez, L., Limarino, C., Martín- González, F., Méndez-Bedia, I., Pedreira, D., Quintana, L., Rodríguez-Fernández, L.R., Rubio-Ordóñez, A., Seggiaro, R., Serra-Varela, S., Spalletti, L., Cardó, R., Ramos, V.A., 2018. Evolución Geodinámica de los Andes argentino-chilenos y la Península Antártica durante el Neoproterozoico tardío y el Paleozoico. Trabajos de Geología 36, 237–278.
Hervé, F., Calderón, M., Faúndez, V., 2008. The metamorphic complexes of the Patagonian and Fuegian Andes. Geol. Acta 6, 43–53.
Hervé, F., Calderon, M., Fanning, C.M., Pankhurst, R.J., Fuentes, F., Rapela, C.W., Correa, J., Quezada, P., Marambio, C., 2016. Devonian magmatism in the accretionary complex of southern Chile. J. Geol. Soc. 173 (4), 587–602.
Hervé, F., Calderón, M., Fanning, M.C., Pankhurst, R.J., Rapela, C.W., Quezada, P., 2018. The country rocks of Devonian magmatism in the North Patagonian Massif and Chaitenia. Andean Geol. 45, 301–317.
Hou, T., Zhang, Z., Keiding, J.K., Veksler, I.V., 2015. Petrogenesis of the ultrapotassic Fanshan intrusion in the North China Craton: implications for lithospheric mantle metasomatism and the origin of apatite ores. J. Petrol. 56, 893–918.
Janoušek, V., Farrow, C.M., Erban, V., 2006. Interpretation of whole-rock geochemical data in igneous geochemistry: introducing Geochemical Data Toolkit (GCDkit). J. Petrol. 47, 1255–1259.
Janoušek, V., Moyen, J.-F., Martin, H., Erban, V., Farrow, C., 2016. Geochemical Modelling of Igneous Processes – Principles and Recipes in R Language. Springer, Berlin Heideberg.
Kemp, A.I.S., Hawkesworth, C.J., Collins, W.J., Gray, C.M., Blevin, P.L., 2009. Isotopic evidence for rapid continental growth in an extensional accretionary orogen: The Tasmanides, eastern Australia. Earth Planet. Sci. Lett. 284 (3-4), 455–466.
Kirsch, M., Paterson, S.R., Wobbe, F., Ardila, A.M.M., Clausen, B.L., Alasino, P.H., 2016. Temporal histories of Cordilleran continental arcs: Testing models for magmatic episodicity. Am. Mineral. 101 (10), 2133–2154.
Li, L., Xiong, X.L., Liu, X.C., 2017. Nb/Ta fractionation by amphibole in hydrous basaltic systems: implications for arc magma evolution and continental crust formation. J. Petrol. 58, 3–28.
Lucassen, F., Trumbull, R., Franz, G., Creixell, C., Vásquez, P., Romer, R.L., Figueroa, O., 2004. Distinguishing crustal recycling and juvenile additions at active continental margins: the Paleozoic to recent compositional evolution of the Chilean Pacific margin (36–41 S). J. S. Am. Earth Sci. 17 (2), 103–119.
Marcos, P., Pavón Pivetta, C., Benedini, L., Gregori, D., Geraldes, M., Scivetti, N., Barros, M., Varela, M., Costa dos Santos, A., 2020. Late Paleozoic geodynamic evolution of the western North Patagonian Massif and its tectonic context along the southwestern Gondwana margin. Lithos 376-377, 105801.
Martin, M.W., Kato, T.T., Rodriguez, C., Godoy, E., Duhart, P., McDonough, M., Campos, A., 1999. Evolution of the late Paleozoic accretionary complex and overlying forearc-magmatic arc, south central Chile (38°–41°S): Constraints for the tectonic setting along the southwestern margin of Gondwana. Tectonics 18 (4), 582–605.
Martínez Dopico, C.I., Tohver, E., López de Luchi, M.G., Wemmer, K., Rapalini, A.E., Cawood, P.A., 2017. Jurassic cooling ages in Paleozoic to early Mesozoic granitoids of northeastern Patagonia: $^{40}Ar/^{39}Ar$, $^{40}K–^{40}Ar$ mica and U-Pb zircon evidence. Int. J. Earth Sci. 106 (7), 2343–2357.
Martínez, J.C., Dristas, J.A., Massonne, H.-J., 2012. Palaeozoic accretion of the microcontinent Chilenia, North Patagonian Andes: high-pressure metamorphism and subsequent thermal relaxation. Int. Geol. Rev. 54 (4), 472–490.
McCarthy, A., Tugend, J., Mohn, G., 2021. Formation of the Alpine orogen by amagmatic convergence and assembly of previously rifted lithosphere. Elements 17, 29–34.
McGee, L.E., Smith, I.E., Millet, M.A., Handley, H.K., Lindsay, J.M., 2013. Asthenospheric control of melting processes in a monogenetic basaltic system: a case study of the Auckland Volcanic Field, New Zealand. J. Petrol, 54, 2125-2153.
McLennan, S.M., 2001. Relationships between the trace element composition of sedimentary rocks and upper continental crust. Geochem. Geophys. Geosyst. 2 (4), n/a–n/a.
Moyen, J.-F., 2009. High Sr/Y and La/Yb ratios: the meaning of the "adakitic signature". Lithos 112 (3-4), 556–574.
Moyen, J.F., Laurent, O., Chelle-Michou, C., Couzinié, S., Vanderhaeghe, O., Zeh, A., Villaros, A., Gardien, V., 2017. Collision vs. subduction-related magmatism: two contrasting ways of granite formation and implications for crustal growth. Lithos 277, 154–177.
Nandedkar, R.H., Hürlimann, N., Ulmer, P., Müntener, O., 2016. Amphibole–melt trace element partitioning of fractionating calc-alkaline magmas in the lower crust: an experimental study. Contrib. Mineral. Petrol. 171, 1–25.
Nelson, D.A., Cottle, J.M., 2018. The secular development of accretionary orogens: linking the Gondwana magmatic arc record of West Antarctica, Australia and South America. Gondwana Res. 63, 15–33.
Nielsen, R.L., Ustunisik, G., Weinsteiger, A.B., Tepley, F.J., Johnston, A.D., Kent, A.J.R., 2017. Trace element partitioning between plagioclase and melt: An investigation of the impact of experimental and analytical procedures. Geochem. Geophys. Geosyst. 18 (9), 3359–3384.
Oriolo, S., González, P.D., Alegre, P., Wemmer, K., Varela, R., Basei, M.A.S., 2023. The Cuesta de Rahue Basement Inlier (Southern Neuquén Precordillera, Argentina): A Devonian to Triassic polyphase orogenic record in northern Patagonia. J. Geol. Soc. https://doi.org/10.1144/jgs2022-143.
Oriolo, S., Schulz, B., González, P.D., Bechis, F., Olaizola, E., Krause, J., Renda, E.M., Vizán, H., 2019. The Late Paleozoic tectonometamorphic evolution of Patagonia revisited: Insights from the pressure-temperature-deformation-time (P-T-D-t) path of the Gondwanide basement of the North Patagonian Cordillera (Argentina). Tectonics 38 (7), 2378–2400.
Pankhurst, R.J., Rapela, C.W., Fanning, C.M., Márquez, M., 2006. Gondwanide continental collision and the origin of Patagonia. Earth-Sci. Rev. 76 (3-4), 235–257.
Pankhurst, R.J., Rapela, C.W., López De Luchi, M.G., Rapalini, A.E., Fanning, C.M., Galindo, C., 2014. The Gondwana connections of northern Patagonia. J. Geol. Soc. 171 (3), 313–328.
Paterson, S.R., Ducea, M.N., 2015. Arc magmatic tempos: Gathering the evidence. Elements 11 (2), 91–98.
Pearce, J.A., 2008. Geochemical fingerprinting of oceanic basalts with applications to ophiolite classification and the search for Archean oceanic crust. Lithos 100 (1-4), 14–48.
Plissart, G., González-Jiménez, J.M., Garrido, L.N., Colás, V., Berger, J., Monnier, C., Diot, H., Padrón-Navarta, J.A., 2019. Tectono-metamorphic evolution of subduction channel serpentinites from South-Central Chile. Lithos 336, 221–241.
Profeta, L., Ducea, M.N., Chapman, J.B., Paterson, S.R., Gonzales, S.M.H., Kirsch, M., Petrescu, L., DeCelles, P.G., 2015. Quantifying crustal thickness over time in magmatic arcs. Sci. Rep. 5, 1–7.
Ramos, V.A., 2008. Patagonia: a Paleozoic continent adrift? J. S. Am. Earth Sci. 26 (3), 235–251.
Ramos, V.A., Cingolani, C., Chemale, F., Naipauer, M., Rapalini, A., 2017. The Malvinas (Falkland) Islands revisited: the tectonic evolution of southern Gondwana based on U-Pb and Lu-Hf detrital zircon isotopes in the Paleozoic cover. J. S. Am. Earth Sci. 76, 320–345.
Rapela, C.W., Pankhurst, R.J., 2020. The continental crust of Northeastern Patagonia. Ameghiniana 57, 480–498.
Rapela, C.W., Hervé, F., Pankhurst, R.J., Calderón, M., Fanning, C.M., Quezada, P., Poblete, F., Palape, C., Reyes, T., 2021. The Devonian accretionary orogen of the North Patagonian cordillera. Gondwana Res. 96, 1–21.
Renda, E.M., 2020. Estudios geológicos y geofísicos a lo largo de una posible faja de deformación entre dominios patagónicos: la sierra de Taquetrén. University of Buenos Aires. PhD Thesis.
Renda, E.M., Alvarez, D., Prezzi, C., Oriolo, S., Vizán, H., 2019. Inherited basement structures and their influence in foreland evolution: a case study in Central Patagonia, Argentina. Tectonophysics 772, 228232.

Renda, E.M., González, P.D., Vizán, H., Oriolo, S., Prezzi, C., Ruiz González, V., Schulz, B., Krause, J., Basei, M., 2021. Igneous-metamorphic basement of Taquetrén Range, Patagonia, Argentina: A key locality for the reconstruction of the Paleozoic evolution of Patagonia. J. S. Am. Earth Sci. 106, 103045.
Romero, R., Barra, F., Leisen, M., Salazar, E., González-Jiménez, J.M., Reich, M., 2020. Sedimentary provenance of the Late Paleozoic metamorphic basement, south-central Chile: Implications for the evolution of the western margin of Gondwana. Int. Geol. Rev. 62 (5), 598–613.
Sawyer, E.W., 1998. Formation and evolution of granite magmas during crustal reworking: the significance of diatexites. J. Petrol. 39 (6), 1147–1167.
Schmidt, M.W., Jagoutz, O., 2017. The global systematics of primitive arc melts. Geochem. Geophys. Geosyst. 18 (8), 2817–2854.
Serra-Varela, S., González, P.D., Giacosa, R.E., Heredia, N., Pedreira, D., Martín González, F., Sato, A.M., 2019. Evolution of the Palaeozoic basement of the North Patagonian Andes in the San Martín de los Andes area (Neuquén, Argentina): petrology, age and correlations. Andean Geol. 46, 102–130.
Serra-Varela, S., Heredia, N., Otamendi, J., Giacosa, R., 2021. Petrology and geochronology of the San Martín de los Andes batholith: Insights into the Devonian magmatism of the North Patagonian Andes. J. S. Am. Earth Sci. 109, 103283.
Shimizu, K., Liang, Y., Sun, C., Jackson, C.R.M., Saal, A.E., 2017. Parameterized lattice strain models for REE partitioning between amphibole and silicate melt. Am. Mineral. 102 (11), 2254–2267.
Spencer, C.J., Kirkland, C.L., Prave, A.R., Strachan, R.A., Pease, V., 2019. Crustal reworking and orogenic styles inferred from zircon Hf isotopes: Proterozoic examples from the North Atlantic region. Geosci. Front. 10 (2), 417–424.
Suárez, R., González, P.D., Ghiglione, M.C., 2019. A review on the tectonic evolution of the Paleozoic-Triassic basins from Patagonia: Record of protracted westward migration of the pre-Jurassic subduction zone. J. S. Am. Earth Sci. 95, 102256.
Sun, S.-s., McDonough, W.F., 1989. Chemical and isotopic systematics of oceanic basalts: implications for mantle composition and processes. Geol. Soc. Spec. Pub. 42 (1), 313–345.
Tang, M., Ji, W.Q., Chu, X., Wu, A., Chen, C., 2021. Reconstructing crustal thickness evolution from europium anomalies in detrital zircons. Geology 49, 76–80.
Varela, R., Basei, M.A.S., Cingolani, C.A., Siga, O., Passarelli, C.R., 2005. El basamento cristalino de los Andes norpatagónicos en Argentina: Geocronología e interpretación tectónica. Rev. Geol. Chile 32, 167–187.
Varela, R., Gregori, D.A., González, P.D., Basei, M.A.S., 2015. Caracterización geoquímica del magmatismo de arco devónico y carbonífero-pérmico en el noroeste de Patagonia, Argentina. Rev. Asoc. Geol. Arg. 72, 419–432.
Vermeesch, P., 2012. On the visualisation of detrital age distributions. Chem. Geol. 312, 190–194.
Vizán, H., Prezzi, C.B., Geuna, S.E., Japas, M.S., Renda, E.M., Franzese, J., Van Zele, M. A., 2017. Paleotethys slab pull, self-lubricated weak lithospheric zones, poloidal and toroidal plate motions, and Gondwana tectonics. Geosphere 13, 1541–1554.
von Gosen, W., 2003. Thrust tectonics in the north Patagonian massif (Argentina): Implications for a Patagonia plate. Tectonics 22 (1), n/a–n/a.
von Gosen, W., 2009. Stages of Late Palaeozoic deformation and intrusive activity in the western part of the North Patagonian Massif (southern Argentina) and their geotectonic implications. Geol. Mag. 146 (1), 48–71.
Young, A., Flament, N., Maloney, K., Williams, S., Matthews, K., Zahirovic, S., Müller, R.D., 2019. Global kinematics of tectonic plates and subduction zones since the late Paleozoic Era. Geosci. Frontiers 10 (3), 989–1013.
Yoya, M.B., Oriolo, S., González, P., Restelli, F., Renda, E., Bechis, F., Newbery, J.C., Marcos, P., Olaizola, E., 2023. The birth of the Gondwanide arc: Insights into Carboniferous magmatism of the North Patagonian Andes (Argentina). J. S. Am. Earth Sci. 123, 104225.
Zamboni, D., Gazel, E., Ryan, J.G., Cannatelli, C., Lucchi, F., Atlas, Z.D., Trela, J., Mazza, S.E., De Vivo, B., 2016. Contrasting sediment melt and fluid signatures for magma components in the Aeolian Arc: Implications for numerical modeling of subduction systems. Geochem. Geophys. Geosyst. 17 (6), 2034–2053.
Zanchetta, S., Garzanti, E., Doglioni, C., Zanchi, A., 2012. The Alps in the Cretaceous: a doubly vergent pre-collisional orogen. Terra Nova 24, 351–356.